Modification of microbial polymers by thiol-ene click reaction: nanoparticle formation and drug encapsulation

Alberto Lanz-Landázuri, Antxon Martínez de Ilarduya, Montserrat García-Alvarez,*
Sebastián Muñoz-Guerra

Departament d'Enginyeria Química, Universitat Politècnica de Catalunya,
ETSEIB, Diagonal 647, 08028, Barcelona, Spain.

*Corresponding author: montserrat.garcia@upc.edu

ABSTRACT

Comb-like amphiphilic polymers were obtained by grafting long paraffinic chains on microbial poly(γ,DL-glutamic acid) and poly(β,L-malic acid) through two steps, *i.e.* allylation of the carboxylic side groups followed by UV-initiated thiol-ene *click* reaction with 1-alkanethiols bearing 8, 12 and 16 carbon atoms, and their characterization was accomplished by ^{1}H NMR, GPC and DSC. The grafted polymers were capable of self-assembling in nanoparticles with diameters in the 80-240 nm range. Incubation in water under physiological conditions led to hydrolysis of the lateral ester bonds followed by scission of the polyamide or polyester main chain. The model drugs, Theophylline and Carbamazepine, were efficiently encapsulated in these systems with much better results attained for the later. Drug release from nanoparticles incubated under physiological conditions occurred with a burst effect and were completely discharged in 24 h. Release profiles recorded from drug-loaded films suggested that the drug was delivered in both cases through a diffusion process.

Keywords: poly(γ-glutamic acid); poly(β,L-malic acid); click-reaction; drug encapsulation; biodegradable nanoparticles.

1. Introduction

Biodegradable polymers are currently of great interest for their use in temporal biomedical applications like chirurgical sutures and drug delivery systems. Among them, biopolymers either of natural occurrence or biotechnologically produced, stand out because they are bioassimilable and biocompatible [1-3]. Poly(γ-glutamic acid) (PGGA) and poly(*β*,L-malic acid) (PMLA) are microbial polymers produced by fermentation with bacteria and fungi respectively, that have been shown to be excellent candidates as biodegradable materials for medical applications.

PGGA can be produced by several species of bacteria of the genus *Bacillus*, classified as GRAS (Generally Regarded As Safe) by the US Food and Drug Administration [4]. It is a water-soluble polyamide that degrades into glutamic acid which is an essential substance to humans [5,6]. PGGA and its derivatives are promising biomaterials that distinguish by being able to display functional properties due to the presence of the carboxylic side group attached to the polyamide main chain [6]. Amphiphilic PGGA derivatives can be produced by chemical modification and some of them have been used to prepare nanoparticles for drug and vaccine delivery system (DDS) [7,8].

PMLA is naturally produced by myxomicetes and filamentous fungi. It is a water soluble polyester very prone to undergo hydrolysis with formation of metabolic L-malic acid [9]. PMLA is also a promising building block for the design of drug delivery systems because its excellent biodegradability and biocompatibility and because its carboxylic functionality [10]. PMLA has been used as a platform in the synthesis of nanocarriers for drug delivery [11-15], as well as a constituent in macromolecular conjugates bearing several functionalities, to treat human brain and breast tumors in mouse models [16,17].

Nowadays, biodegradation and bioresorption are considered as prerequisites of any high molecular weight biomaterial that is to be used in human therapy [11]. This has stimulated the modification of naturally occurring biopolymers [18,19], as it is the case of PGGA and PMLA, where the carboxylic groups make their derivatization feasible for the modulation of polymer hydrophobicity and properties [20,21], and for the introduction of bioactive ligands required for the stable association with drugs and their controlled release [5,22]. Graft copolymers consisting of hydrophilic and hydrophobic segments are capable of self-assembling in aqueous solutions to form micro or nanoparticles [13,23]. DDS based on polymer particles are clearly advantageous

because they can effectively deliver the drug to a target site and thus increase the therapeutic benefit, while minimizing side effects. For instance, polymer particles help to increase the stability of drug [3, 24-26].

The concept of functionalization by postpolymerization strategies makes use of modern techniques based on *click* chemistry [27]. In this context, the thiol-ene reaction is particularly attractive because in addition to be facile and versatile, it results in a stable linkage and exhibits minimal cross-reactivity with other functional groups. Morever, this reaction may be performed to near completion under mild conditions giving rise to products that are free of appreciable amounts of impurities [28]. In this work we will take benefit from the functionality of PGGA and PMLA for building amphiphilic comb-like polymers suitable for their application as DDS. PGGA and PMLA are functionalized through a two-step procedure based on the thiol-*ene* reaction. In the first step, the allyl group is introduced by direct esterification, which leads to a double-bond functionalized polymer with potential for further specific modification [29]. In the second step, aliphatic long chains are grafted by *thiol-ene* click-reaction in order to obtain the comb-like architecture required for nanoparticle formation and drug encapsulation. Drugs tested for encapsulation and drug delivery assays were Theophylline and Carbamazepine which are considered as hydrophilic and hydrophobic drug models, respectively.

2. Experimental

2.1. Materials

Polymers used in this work were biotechnologically produced. PGGA was obtained by fermentation of *Bacillus licheniformis,* which was kindly supplied by Dr. Kubota of Meji Co. (Japan). It had a weight-averaged molecular weight of ~30 kDa. PMLA was obtained by fermentation of *Physarum polycephalum,* isolated and purified as described elsewhere [9]. It had a weight-averaged molecular weight of ~25 kDa. Purity of the both PGGA and PMLA samples was ascertained by 300 MHz ^{1}H NMR. Allyl alcohol, allyl bromide, 1-octanethiol, 1-dodecanethiol, 1-hexadecanethiol, 2,2-dimethoxy-2-phenylacetophenone (DMPA), dicyclohexylcarbodiimide (DCC) and Theophylline (1,3-dimethylxanthine, THEO) were acquired from SIGMA-Aldrich, while Carbamazepine (5H-dibenz[b,f]azepine-5-carboxamide, CBZ) was obtained from AKSci (USA). All organic solvents were analytical grade and used without further purification.

2.2. Esterification reactions

Esterification of PGGA with allyl bromide was carried out following the procedure described elsewhere for alkyl-bromides [30]. Briefly, $NaHCO_3$ (525 mg) was added to a solution of 200 mg of PGGA in 20 mL of *N*-methylpyrrolidone (NMP) heated at 60 °C. Allyl bromide was slowly added in the amount required to reach the desired conversion. The reaction was left to proceed for 48 h and the esterified polymer was recovered by precipitation in diethyl ether, washed with acetone, and dried in vacuum for storage.

Esterification of PMLA with allyl alcohol was performed through activation of the carboxyl side group with DCC. Briefly, a mixture of 0.5 or 0.75 mmol of DCC in 2 mL of allyl alcohol was added dropwise to a solution of 1 mmol of PMLA in 2 mL of allyl alcohol; the reaction was left to proceed for 3 h at room temperature under vigorous magnetic stirring. The final reaction mixture was subjected to dialysis against methanol for 48 h using an 8 kDa cut-off membrane. The allyl ester of PMLA was lyophilized for recovery and storage.

2.3. Thiol-ene click reactions

The PGGA and PMLA 3-alkylthio-propyl esters (*co*PGGA-PrSR_xH_y and *co*PMLA-PrSR_xH_y) were prepared as follows: To a 7.5 % (w/v) solution of the PGGA allyl ester in NMP at room temperature, the corresponding 1-alkanethiol (1-octanethiol, 1-dodecanethiol, 1-hexadecanethiol) was added in a 2:1 molar ratio respect to double bond concentration, and then DMPA (4 %-mol respect to double bond) was added. The reaction mixture was placed in an UV lamp (2 x Philips PL-S 11 W/10, 360 nm) and it was irradiated for 24 h after which the reaction was completed according to ^{1}H NMR. The grafted PGGA was recovered by pouring the reaction mixture into ethanol and the product was dried in vacuum for storage. The same procedure was applied for the preparation of the PMLA derivatives but starting from a solution of 1.5 % (w/v) of the PMLA allyl ester in DMSO.

2.4. Particles formation and drug encapsulation

Precipitation-dialysis was found to be a suitable procedure to produce nanoparticles due to the capacity of the amphiphilic copolymers, *co*PGGA-PrSR_xH_y and *co*PMLA-PrSR_xH_y to self-assemble in layered nanostructures. Briefly, 1 mL of water was added dropwise to a 1 mL of 1 % solution of *co*PGGA-PrSR_xH_y in NMP or to 1 mL of 0.25 % solution of *co*PMLA-PrSR_xH_y in DMSO, in both cases under magnetic stirring.

Mixtures were dialyzed against distilled water for 24 h using a cellulose membrane of 8 kDa M_w cut-off. Particles morphology was examined by SEM and their average hydrodynamic diameters and ζ potential were determined by light scattering. NPs were recovered by centrifugation freeze-dried. The same procedure was used for the preparation of the nanoparticles encapsulated with THEO or CBZ but using drug-saturated water for the dialysis process. The drugs were added at a concentration of 20 % (w/w) with respect to polymer in the organic solution. Samples were recovered by centrifugation, washed with distilled water and freeze-dried for storage.

2.5. Hydrolytic degradation

Hydrolytic degradation was studied by following the reduction in molecular weight as a function of incubation time. For this, fresh nanoparticles suspensions containing 2.5 mg of nanoparticles in 1 mL of phosphate buffer pH 7.4 were prepared and incubated at 37 °C. Samples were frozen at scheduled times and analyzed by GPC. The hydrolytic degradation mechanism was examined by means of ^{1}H NMR by monitoring the changes taking place in the mother solution along the degradation process. For this, 10 mg of nanoparticles were resuspended in 1 mL of deuterated phosphate buffer pH 7.4 with D_2O and placed in NMR tubes, and ^{1}H NMR spectra were recorded at scheduled times.

2.6. Drug-loaded films

Drug-loaded films were prepared by casting. Briefly, 1 mL of 2 % (w/v) solution of either PGGA or PMLA copolymer in $CHCl_3$ and 0.5 mL of 0.4 % (w/v) solution of CBZ in $CHCl_3$ were mixed and slowly evaporated on a Teflon sheet. Films containing THEO were not prepared because no common solvent for polymers and drug could be found. DSC analysis was performed on drug-loaded films to determine the crystalline state of the drug in the films.

2.7. In vitro drug release

In vitro drug release of Theophylline and Carbamazepine from the loaded polymer was evaluated by the dialysis method. Briefly, 10 mg of drug loaded nanoparticles were resuspended in 1 mL of phosphate buffer pH 7.4, and transferred into a dialysis tube with 8 kDa molecular weight cut-off. The tube was then immersed into 20 mL of buffer and placed under incubation at 37 °C. 2 mL aliquots of the releasing medium were taken at scheduled times, and the drawn volume replaced by fresh buffer. Drug

concentration was determined by UV spectroscopy at 220 and 275 nm for CBZ and THEO, respectively. The amount of drug loaded on the particles $[drug]_{np}$ was determined by dissolving the particles in the appropriate solvent (DMSO, MeOH or DCM) and measuring the drug concentration by UV-vis spectrophotometry using a calibration curve built with the free drug. Encapsulation efficiency (EE) was calculated on the basis of the following formula:

$$\%EE = \frac{[drug]_{np}}{[drug]_i} 100$$

where $[drug]_i$ is the drug concentration relative to polymer (w/w) in the initial solution. Cumulative drug release was calculated as a function of time. The same procedure was employed for CBZ release from films.

2.8. Measurements

NMR spectra were recorded on a Bruker AMX-300 instrument from samples dissolved either in DMSO-d_6 or $CDCl_3$ containing minor amounts of trifluoroacetic acid. Degradation products were analyzed in the same aqueous buffer used for incubation using D_2O instead of H_2O. ^1H NMR spectra where recorded at 25 °C operating at 300.1 MHz; 128 scans were acquired with 32K data points and relaxation delays of 2 seconds. UV spectrophotometry was performed in a UV-visible spectrophotometer CECIL CE 2021. Gel permeation chromatography (GPC) was done using a Waters 515 HPLC pump provided with a Waters 410 differential refractometer detector and a Waters Styragel HR 5E column (7.8 x 300 mm) (Waters, Massachusetts, USA). Samples were chromatographed using 0.05 M sodium trifluoroacetate in hexafluoroisopropanol at 0.5 $mL \cdot min^{-1}$ flow rate. Chromatograms were calibrated against poly(methyl methacrylate) standards (Varian, USA). DSC analysis was made using a Perkin-Elmer Pyris 1 apparatus. Thermograms were obtained from 2-4 mg samples at heating and cooling rates of 10 $°C \cdot min^{-1}$, under nitrogen flow. Indium and zinc were used as standards for temperature and enthalpy calibrations.

3. Results and discussion

3.1. Comb-like polymers synthesis

Comb-like copolymers from PGGA and PMLA were obtained by a two-step process (Scheme 1). First, polymers were allylated at various degrees using specific procedures for PGGA and PMLA according to the different susceptibility towards hydrolysis displayed by their main chains. PGGA was esterified with allyl bromide under middle-basic conditions whereas allyl alcohol was used for esterifying PMLA with the concourse of DCC as carboxylic activator. Results for the allylation reaction are collected in Table 1. The degree of esterification (%-mol) was determined by integration and relative quantification of the ^{1}H NMR signals arising from the main polymer chain (CH signal appearing in the 4.2-4.3 or 5.2-5.4 ppm range for PGGA or PMLA derivatives, respectively) and the allyl side group OCH_2 signal appearing at 4.7 ppm. Reaction yields were between 88 and 96% for PGGA and between 75 and 80% for PMLA.

<Insert Scheme 1>

<Insert Table 1>

The resulting allylated copolymers were spectroscopycally pure as it was proved by ^{1}H NMR. In fact, the occurrence of allylation of polyacids was clearly evidenced by following the changes taking place in the ^{1}H NMR spectra (Figures 1 and 2). For PGGA the signal of the allylic CH_2 appearing at 4.1 ppm in allyl bromide (spectrum 1b, signal *e*) shifted 0.5 ppm downfield in *co*PGGA-$Al_{50}H_{50}$ (spectrum 1c, signal *e*'). In the case of PMLA, a similar displacement was observed for the allylic CH_2 signal which moved 0.7 ppm downfield when the allyl alcohol entered in the PMLA as alcohyl group (signal *c* in spectrum b compared to signal *c*' in spectrum 2c). Molecular weights were found to increase proportionally to the esterification degree, while copolymers polydispersities displayed similar values for the two copolymer series.

<Insert Figure 1 and 2>

Grafting of the three linear 1-alkanethiols containing 8 (Oc), 12 (dD) and 16 (hD) carbon atoms on allyl functionalized polymers was successfully achieved taking advantage of the high reactivity and specificity of the thiol-ene *click* reaction. DMPA was chosen as photoiniciator and UV radiation as activator. The reaction is known to take place as a free radical reaction initiated by decomposition of DMPA and to proceed with propagation to terminate by radical chain transfer [31]. Conversion degree for all copolymers was practically 100% as it could be assessed by ^{1}H NMR. In fact proton

signals arising from the double bound (5-6 ppm) fully disappeared after reaction (spectra 1d and 2d in Figure 1 and 2, respectively), indicating that the totality of allyl groups had been converted. Nevertheless, reactions yields were relatively lower than for the first step, *i.e.* between 60 and 80% for PGGA and around 45% for PMLA derivatives (Table 2). Losses could be due in part to photodegradation taking place by the prolonged exposition of the polymer to UV radiation. Shorter exposition times were assayed but then reaction did not reach completeness. Such degradation was reflected in the molecular weights of the grafted copolymers which were found to be slightly lower than those of their respective allylated precursors. Nevertheless, M_w values for the three alkylated derivatives coming from each copolymer composition were consistent with the length of the alkylthiol used for grafting at each case (Table 2).

<Insert Table 2>

3.2. Thermal characterization

A DSC calorimetric study was carried out in order to appraise the crystalline character of the grafted copolymers since previous works on similar comb-like systems had shown that long linear alkyl side chains are able to crystallize in a phase separated from that containing the main chains [21]. As it is observed in Figure 3, only copolymers bearing the hexadecyl group displayed endothermal peaks characteristic of melting, and this happens for both PGGA and PMLA and for whichever composition. In all cases, the melting temperature was in the 40-60 ºC range, which is a value fully consistent with what should be expected for the melting of a paraffinic crystal made of alkyl chains of sixteen carbon atoms. Note that multiple melting peaks are observed in some of these DSC traces which could be attributed to the occurrence of multiple crystallite populations differing in size. This is a phenomenon commonly taking place upon polymer crystallization. It is interestingly noticed that peak multiplicity becomes more evident for 50% copolymer compositions suggesting that it is influenced by the density of alkyl side chains. These results are in agreement with what has been reported for poly(α-alkyl-γ-glutamate)s which were found to be able to crystallize only for alkyl chains containing at least 14 carbon atoms [21]. It can be concluded therefore that the sulphur atom is unable to enter in the paraffinic crystal lattice and consequently the thiotrimethylene group must remain in a disordered interphase connecting the alkyl side chains to the backbone of the polypeptide or polyester chains through the carboxylate group.

<Insert Figure 3 >

3.3. Nanoparticles formation and characterization

The amphiphilic polymers created by esterification were capable to spontaneously form self-assembled nanostructures when the precipitation dialysis method was applied. More or less spherical nanoparticles were obtained for *co*PGGA-Pr$SR_{50}H_{50}$, *co*PGGA-Pr$SR_{75}H_{25}$, *co*PMLA-Pr$SR_{50}H_{50}$ and *co*PMLA-Pr$SR_{75}H_{25}$ (Figure 4 and 5), whereas *co*PGGA-Pr$SR_{25}H_{75}$ failed to form particles under the applied conditions. Average hydrodynamical diameters of these particles oscillated from 80 to 240 nm (Table 3), with smaller sizes corresponding to PGGA derivatives. Although there is not apparent correlation between composition and size, a general observation is that polymers containing hexadecyl chains produced the smallest particles, which is probably due to the contraction implied in the crystallization that takes place in these systems.

<Insert Figure 4 and 5>

Particle surface charge was estimated by measuring the ζ-potential in distilled water and results are included in Table 3. Nanoparticles displayed negative charge values according to the presence of free carboxylic groups present in the copolymers derived from both PGGA and PMLA. On the basis of well-settled amphiphilic self-assembled particle structure concept it can be reasonably assumed that the carboxylic grafted chains are hidden in the inner part to form a core-shell structure. The negative charge decreases with increasing conversion degree, which is in accordance with what should be expected for the variation in the negative hydrophilic/neutral hydrophobic ratio. It is noteworthy that the observed differences are higher for PMLA derivatives, which is probably due to the greater ability of the flexible polymalate chain to be sterically accommodated in the particle.

<Insert Table 3>

3.4. Hydrolytic degradation

The hydrolytic degradation of the nanoparticles was examined upon incubation in water under physiological conditions, *i.e.* pH 7.4 and 37 °C (Figure 6). Degradation rate was determined by following the molecular weight reduction as a function of incubation time. As it was expected the susceptibility of nanoparticles to hydrolysis decreased for higher conversion degrees and longer alkyl side chain lengths. Both factors, esterififcation degree and lateral chain length, are directly related to the material

hydrophobicity, and therefore to the sensitiveness to hydrolysis of the copolymers. PMLA copolymer derivatives displayed a much higher rate of hydrolysis than those of PGGA because the greater lability of the main chain ester bond compared to the amide bond. The degradation profiles depicted in Figure 6 show that after 12 weeks of incubation, *co*PGGA-PrSOc$_{50}$H$_{50}$ retained about 60 % of its original molecular weight, while for *co*PGGA-PrShD$_{50}$H$_{50}$ the value was above 80 %. Conversely, in PMLA derivatives, the *co*PMLA-PrSOc$_{50}$H$_{50}$ molecular weight fell down to 35 % of its original value while for *co*PMLA-PrShD$_{50}$H$_{50}$ it remained around 70 %. The hydrolysis rate of polymers with 75% of modified units was significantly slower so that only those containing the octyl group showed a considerable molecular weight reduction upon incubation whereas those bearing longer side chains retained more than 90% of their original molecular weight.

<Insert Figure 6>

The hydrolysis mechanism was studied with the support of ^{1}H NMR analysis of the soluble products that are released to the aqueous medium upon incubation. According to the results found in the degradation rate assays, copolymers modified at lower conversion degrees with shorter alkyl side chains degraded considerably faster and PGGA series were more resistant than the PMLA ones. Nevertheless the degradation mechanism seems to be common to all of them. Since *co*PGGA-PrSOc$_{50}$H$_{50}$ and *co*PMLA-PrSOc$_{50}$H$_{50}$ were the most degraded samples in the PGGA and PMLA copolyesters series respectively, and their degradation products are water-soluble, they were chosen to study the degradation mechanism operating in each series. First detectable ^{1}H NMR signals in the degradation of *co*PGGA-PrSOc$_{50}$H$_{50}$ appeared after one month of incubation (Figure 7). They were assigned to protons attached to the main chain carbons of glutamyl residues and to the protons of the alkylthioalkanol revealing the hydrolysis of the ester side group with subsequent solubilization of PGGA fragments enriched in free carboxylic groups. After two months of degradation, end group signals indicative of hydrolysis of the amide bonds from the main chain started to be observable. From the third month ahead, these signals increased in intensity and those arising from the main chain displayed much better resolution. Although formation of free glutamic acid as final degradation product is expected, the presence of this compound in the aqueous medium could not be ascertained because overlapping of its signals with those arising from both polymer and oligomer species.

<Insert Figure 7>

For PMLA derivatives the mechanism was found to be similar although degradation happened faster (Figure 8). In this case, first signals appeared just after one week of incubation and they corresponded to the protons of free malic acid and the hydrolyzed side chain, indicating that hydrolysis of ester groups, in both main chain and side chain, took place at the same time. Upon longer times of incubation no signals arising from terminal groups or main chain malate units were observed in the aqueous solution which is taken as indicative of the non-solubility of the copolymer fragments. After several weeks, spectra became simplified and signals appeared intensified so that at the end of the incubation period, the only visible signals were those arising from free malic acid and the released alkylthioalkanol.

<Insert Figure 8>

3.5. Drug encapsulation and in vitro release

Carbamazepine (CBZ) and Theophylline (THEO) were used as model compounds for hydrophobic and hydrophilic drugs, respectively, for both encapsulation and releasing studies. The encapsulation method applied in this work was the same precipitation dialysis method used for nanoparticle formation but adding the drug to the polymer solution prior to nanoparticle formation. Results obtained for the two drugs in the two series of copolymers are summarized in Table 3. It is apparent that CBZ is able to accommodate much better in the nanoparticles than THEO showing considerable higher encapsulation efficiency (EE) in all cases. The lower encapsulation efficiency found for THEO compared to CBZ may be merely a consequence of greater drug losses occurring at the dialysis stage caused by its higher water affinity.

In vitro drug release assays were carried out under physiological conditions, *i.e.* pH 7.4 and 37 °C and results are depicted in Figure 9. Both drugs displayed a burst release within the first hours of incubation, a fact that was more pronounced for encapsulated THEO nanoparticles, which discharged about 60-80 % of the loaded drug in the first two hours of incubation. CBZ loaded nanoparticles showed a more sustained release needing about six hours to liberate 50% of the encapsulated drug. From these results it can be inferred that differences in releasing rates must be mainly determined by the hydrophobicity of the encapsulated compound. Given both the higher encapsulation efficiency attained for CBZ and the more sustained release displayed by this drug, it can be concluded that the derivatives examined in this work are more suitable for the design of DDS systems loaded with hydrophobic drugs.

<Insert Figure 9>

To understand the process governing drug release in the nanoparticles, CBZ loaded-films of both PGGA and PMLA copolymers were prepared and subjected to release assays. To get insight of the state of CBZ in the films, they were analyzed by DSC and compared to both those made of pure polymer and the blends prepared by physical mixing of the polymer and the drug. As it is seen in Figure 10, the DSC trace of CBZ showed a characteristic melting peak at 180-190 °C, which was also present in traces recorded from the physical blends but not from drug-loaded films, suggesting that the drug became well dispersed in the polymeric matrix. Incubation of the drug-loaded films showed that, although releasing happened at slower rates than for nanoparticles, the drug became almost completely liberated in the first two days (Figure 11). Furthermore, release rates were faster for films made of copolymers with lower modification degrees and bearing shorter aliphatic chains. Again drug release has to be related to the hydrophobicity of the material and water penetration capability. Given the similitude of behavior observed for films and nanoparticles, it can be reasonably assumed that the same diffusion process must govern drug release in both systems. The conclusion is therefore that drug release of CBZ from these materials must be governed by a diffusion process since degradation of the copolymers requires much longer periods of time.

<Insert Figure 10 and 11>

4. Conclusions

Microbial polymalic and polyglutamic acids were modified by grafting long alkyl chains through a two-step process that makes use of thiol-ene *click* reactions. The prepared amphiphilic copolymers were able to self-assemble in aqueous media into nanostructurated particles with diameters within the 80- 240 nm range, the smaller ones being those prepared from PGGA derivatives. These nanoparticles were degraded by hydrolysis under physiological conditions at a rate faster for PMLA than for PGGA derivatives as correspond to differences expected between polyesters and polyamides. Degradation happened by releasing the corresponding thioether alcohol and either malic or glutamic acid to the medium. THEO and CBZ were encapsulated in the polymer nanoparticles with better efficiency for the hydrophobic drug CBZ than for the hydrophilic THEO. Both drugs were released upon incubation of the nanoparticles in water at pH 7.4 and 37 $^{\circ}$C displaying a burst release in the first few hours to reach

almost completion after 24 h of incubation. The CBZ release profile obtained from drug-loaded films suggested that the drug was liberated through a mediated-diffusion process.

Acknowledgments

This work received financial support from MCINN of Spain with Grants MAT2009-14053-C02-01 and MAT2012-38044-C03-03 and from AGAUR with grant 2009SGR1469. Thanks also to AGAUR (Generalitat de Catalunya) for the Ph.D. grant awarded to Alberto Lanz.

References

[1] B.S. Lee, M. Vert, E. Holler, Water-soluble Aliphatic Polyesters: Poly(malic acid)s, in: Biopolymers Online: Wiley-VCH Verlag GmbH & Co. KGaA; 2005.

[2] V. Hasirci, K. Lewandrowski, J.D. Gresser, D.L. Wise, D.J. Trantolo, Versatility of biodegradable biopolymers: degradability and an in vivo application, J. Biotechnol. 86 (2001) 135-150.

[3] B. Manocha, A. Margaritis, Production and characterization of gamma-polyglutamic acid nanoparticles for controlled anticancer drug release, Crit. Rev. Biotechnol. 28 (2008) 83-99.

[4] A. Pacini, M. Caricato, S. Ferrari, D. Capsoni, A. Martínez de Ilarduya, S. Munoz-Guerra, D. Pasini, Poly(gamma-glutamic acid) esters with reactive functional groups suitable for orthogonal conjugation strategies, J. Polym. Sci. Pol. Chem. 50 (2012) 4790-4799.

[5] L.L. Wang, Y.X. Wu, R.W. Xu , G.Y. Wu, W.T. Yang, Synthesis and characterization of poly(L-glutamic acid-co-L-aspartic acid), Chinese J. Polym. Sci. 26 (2008) 381-391.

[6] S. Muñoz-Guerra, M. García-Alvarez, J.A. Portilla-Arias, Chemical Modification of Microbial Poly(g-glutamic acid): Progress and Perspectives, J. Renew. Mater. 1 (2013) 42-60.

[7] A. Richard, A. Margaritis, Poly(glutamic acid) for biomedical applications, Crit. Rev. Biotechnol. 21 (2001) 219-232.

[8] I.L. Shih, Y.T. Van, M.H. Shen, Biomedical applications of chemically and microbiologically synthesized poly(glutamic acid) and poly(lysine), Mini Rev. Med. Chem. 4 (2004) 179-188.

[9] E. Holler, Poly(malic Acid) from Natural Sources, in: N.P. Cheremisinoff (Ed.), Handbook of Engineering Polymeric Materials, Marcel Dekker, USA, 1997, pp. 93-103.

[10] E. Holler, B.S. Lee, Analysis of poly(β-L-malic acid) in tissue and solution, Recent. Res. Devel. Anal. Chem. 2 (2002) 177-192.

[11] K. Abdellaoui, M. Boustta, M. Vert, M. Manfait, Metabolite-derived artificial polymers designed for drug targeting, cell penetration and bioresorption, Eur. J. Pharm. Sci. 6 (1998) 61-73.

[12] S. Osanai, K. Nakamura, Effects of complexation between liposome and poly(malic acid) on aggregation and leakage behaviour, Biomaterials 21 (2000) 867-876.

[13] S. Cammas-Marion, M.M. Bear, A. Harada, P. Guerin, K. Kataoka, New macromolecular micelles based on degradable amphiphilic block copolymers of malic acid and malic acid ester, Macromol. Chem. Phys. 201 (2000) 355-364.

[14] J.A. Portilla-Arias, M. García-Alvarez, A. Martínez de Ilarduya, E. Holler, J.A. Galbis, S. Muñoz-Guerra, Synthesis, degradability, and drug releasing properties of methyl esters of fungal poly(beta,L-malic acid), Macromol. Biosci. 8 (2008) 540-550.

[15] A. Lanz-Landázuri, M. García-Alvarez, J. Portilla-Arias, A. Martínez de Ilarduya, E. Holler, J.Y. Ljubimova, S. Muñoz-Guerra, Modification of Microbial Polymalic Acid With Hydrophobic Amino Acids for Drug-Releasing Nanoparticles, Macromol. Chem. Phys. 213 (2012) 1623-1631.

[16] B.S. Lee, M. Fujita, N.M. Khazenzon, K.A. Wawrowsky, S. Wachsmann-Hogiu, D.L. Farkas, K.L. Black, J.Y. Ljubimova, E. Holler, Polycefin, a new prototype of a multifunctional nonconjugate based on poly(beta-L-malic acid) for drug delivery, Bioconjugate Chem. 17 (2006) 317-326.

[17] J.Y. Ljubimova, M. Fujita, A.V. Ljubimov, V.P. Torchilin, K.L. Black, E. Holler, Poly(malic acid) nanoconjugates containing various antibodies and oligo nucleotides for multitargeting drug delivery, Nanomedicine 3 (2008) 247-265.

[18] M.E. Martínez Barbosa, S. Cammas, M. Appel, G. Ponchel, Investigation of the degradation mechanisms of poly(malic acid) esters in vitro and their related cytotoxicities on J774 macrophages, Biomacromolecules 5 (2004) 137-143.

[19] O. Coulembier, P. Degée, J.L. Hedrick, P. Dubois, From controlled ring-opening polymerization to biodegradable aliphatic polyester: Especially poly(beta-malic acid) derivatives, Prog. Polym. Sci. 31 (2006) 723-747.
[20] C.E. Fernández, M. Mancera, E. Holler, J.A. Galbis, S. Muñoz-Guerra, High molecular weight methyl ester of microbial poly(beta,L-malic acid): Synthesis and crystallization Polymer 47 (2006) 6501-6508.
[21] M. Morillo, A. Martínez de Ilarduya, S. Muñoz-Guerra, Comblike alkyl esters of biosynthetic poly(gamma-glutamic acid). 1. Synthesis and characterizationm, Macromolecules 34 (2001) 7868-7875.
[22] B. Manocha, A. Margaritis, Controlled Release of Doxorubicin from Doxorubicin/gamma-Polyglutamic Acid Ionic Complex.J. Nanomater. 2010 (2010) 1-9.
[23] J.A. Portilla-Arias, B. Camargo, M. García-Alvarez, A. Martínez de Ilarduya, S. Muñoz-Guerra, Nanoparticles Made of Microbial Poly(gamma-glutamate)s for Encapsulation and Delivery of Drugs and Proteins, J. Biomat. Sci-Polym. E. 20 (2009) 1065-1079.
[24] V.J. Mohanraj, Y. Chen, Nanoparticles - A Review Trop. J. Pharm. Res. 5 (2006) 561-573.
[25] A.S. Hoffman, The origins and evolution of "controlled" drug delivery systems, J. Control. Release 132 (2008) 153-163.
[26] Y. Malam, M. Loizidou, M. A. Seifalian, Liposomes and nanoparticles: nanosized vehicles for drug delivery in cancer.Trends Pharmacol. Sci. 30 (2009) 592-599.
[27] L.M. Campos, K.L. Killops, R. Sakai, J.M.J. Paulusse, D. Damiron, E. Drockenmuller, B.W. Messmore, C.J. Hawker, Development of thermal and photochemical strategies for thiol-ene click polymer functionalization, Macromolecules 41 (2008) 7063-7070.
[28] C.E. Hoyle, A.B. Lowe, C.N. Bowman, Thiol-click chemistry: a multifaceted toolbox for small molecule and polymer synthesis, Chem. Soc. Rev. 39 (2010) 1355-1387.
[29] C.H. Wong, S.C. Zimmerman, Orthogonality in organic, polymer, and supramolecular chemistry: from Merrifield to click chemistry, Chem. Commun. 49 (2013) 1679-1695.
[30] R.A. Gross, S.P. McCarthy, D.T. Shah, γ-poly(glutamic acid) esters, patent U. (Ed.), USA, 1995.
[31] S.P.S. Koo, M.M. Stamenovic, R.A. Prasath, A.J. Inglis, F.E. Du Prez, C. Barner-Kowollik, W. Van Camp, T. Junkers, Limitations of Radical Thiol-ene Reactions for Polymer-Polymer Conjugation, J. Polym. Sci. Pol. Chem. 48 (2010) 1699-1713.

Captions to figures

Scheme 1. Two-step grafting of aliphatic long chains into: a) PGGA and b) PMLA.

Figure 1. ^{1}H NMR spectra of: a) PGGA, b) allyl bromide, c) *co*PGGA-$Al_{50}H_{50}$ and d) *co*PGGA-$PrSOc_{50}H_{50}$. *DMSO-d_5H/H_2O.

Figure 2. ^{1}H NMR spectra: a) PMLA, b) allyl alcohol, c) *co*PMLA-$Al_{50}H_{50}$ and d) *co*PMLA-$PrSOc_{50}H_{50}$. *DMSO-d_5H/H_2O.

Figure 3. DSC traces (first heating) of *co*PGGA-$PrSR_xH_y$ a) and *co*PMLA-$PrSR_xH_y$ b) with alkyl groups containing 8 (Oc), 12 (doD) and 16 (hD) carbon atoms, as indicated.

Figure 4. SEM micrographs of modified PGGA nanoparticles: a) *co*PGGA-$PrSOc_{50}H_{50}$, b) *co*PGGA-$PrSdD_{50}H_{50}$, c) *co*PGGA-$PrShD_{50}H_{50}$, d) *co*PGGA-$PrSOc_{75}H_{25}$, e) *co*PGGA-$PrSdD_{75}H_{25}$ and f) *co*PGGA-$PrShD_{75}H_{25}$.

Figure 5. SEM micrographs of modified PMLA nanoparticles: a) *co*PMLA-$PrSOc_{50}H_{50}$, b) *co*PMLA-$PrSdD_{50}H_{50}$, c) *co*PMLA-$PrShD_{50}H_{50}$, d) *co*PMLA-$PrSOc_{75}H_{25}$, e) *co*PMLA-$PrSdD_{75}H_{25}$ and f) *co*PMLA-$PrShD_{75}H_{25}$.

Figure 6. Evolution of the molecular weight of copolymers incubated under physiological conditions a) *co*PGGA-$PrSR_xH_y$ and b) *co*PMLA-$PrSR_xH_y$.

Figure 7. Evolution of the ^{1}H NMR spectrum recorded from *co*PGGA-$PrSOc_{50}H_{50}$ nanoparticles incubated in aqueous medium at pH 7.4 and 37 ºC.

Figure 8. Evolution of the ^{1}H NMR spectrum recorded from *co*PMLA-$PrSOc_{50}H_{50}$ nanoparticles incubated in aqueous medium at pH 7.4 and 37 ºC.

Figure 9. Drug release profiles for *co*PGGA-$PrSR_xH_y$ (top) and *co*PMLA-$PrSR_xH_y$ (bottom) nanoparticles incubated under physiological conditions and loaded with Carbamazepine (a, a') and Theophylline (b, b').

Figure 10. DSC heating traces of a) pristine polymer, b) physical blend (polymer + CBZ), and c) CBZ loaded film. Left: *co*PGGA-$PrSR_xH_y$;; Right: *co*PMLA-$PrSR_xH_y$. For comparison, the trace of CBZ is included in the bottom of each set.

Figure 11. Carbamazepine release from drug-loaded films. a) *co*PGGA-$PrSR_xH_y$ and b) *co*PMLA-$PrSR_xH_y$.

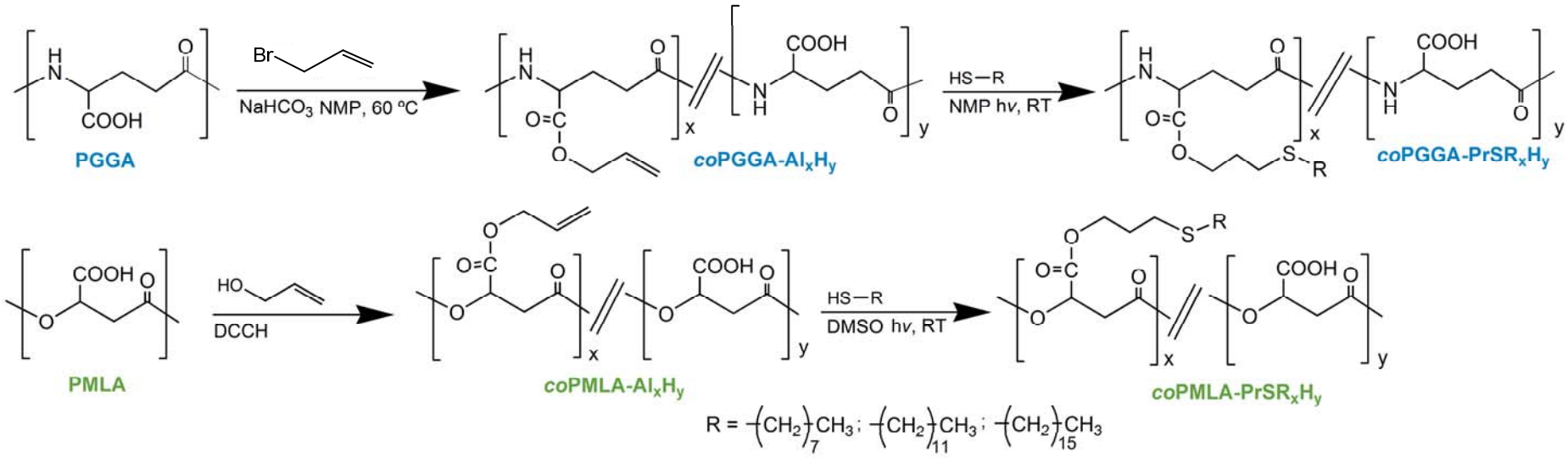
PGGA
NaHCO3 NMP, 60 °C
coPGGA-AIxHy
HS—R
NMP hν, RT
coPGGA-PrSRxHy
PMLA
HO
DCCH
coPMLA-AIxHy
HS—R
DMSO hν, RT
coPMLA-PrSRxHy
R = (CH2)7CH3 ; (CH2)11CH3 ; (CH2)15CH3

Scheme 1

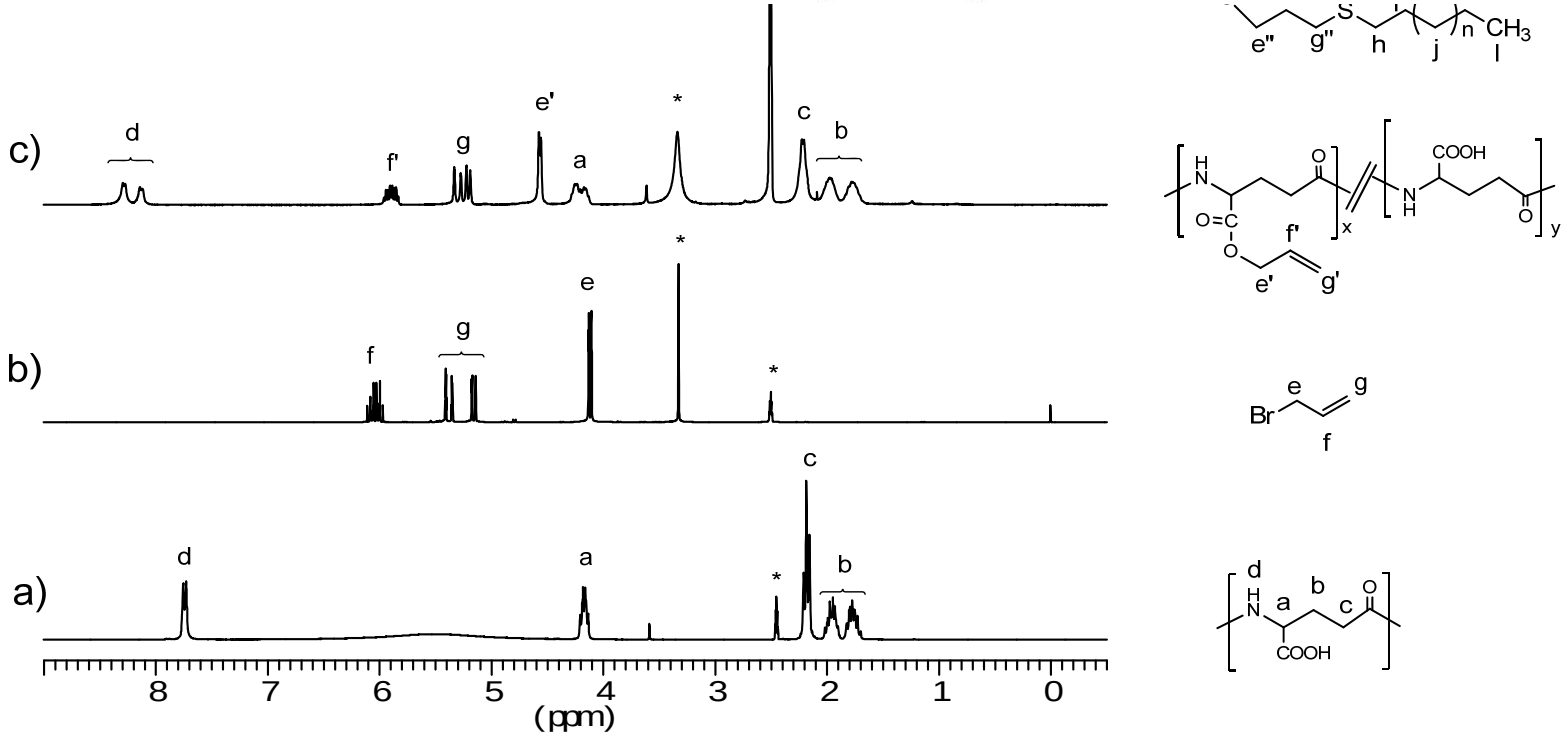
c)
b)
a)
(ppm)

Figure 1

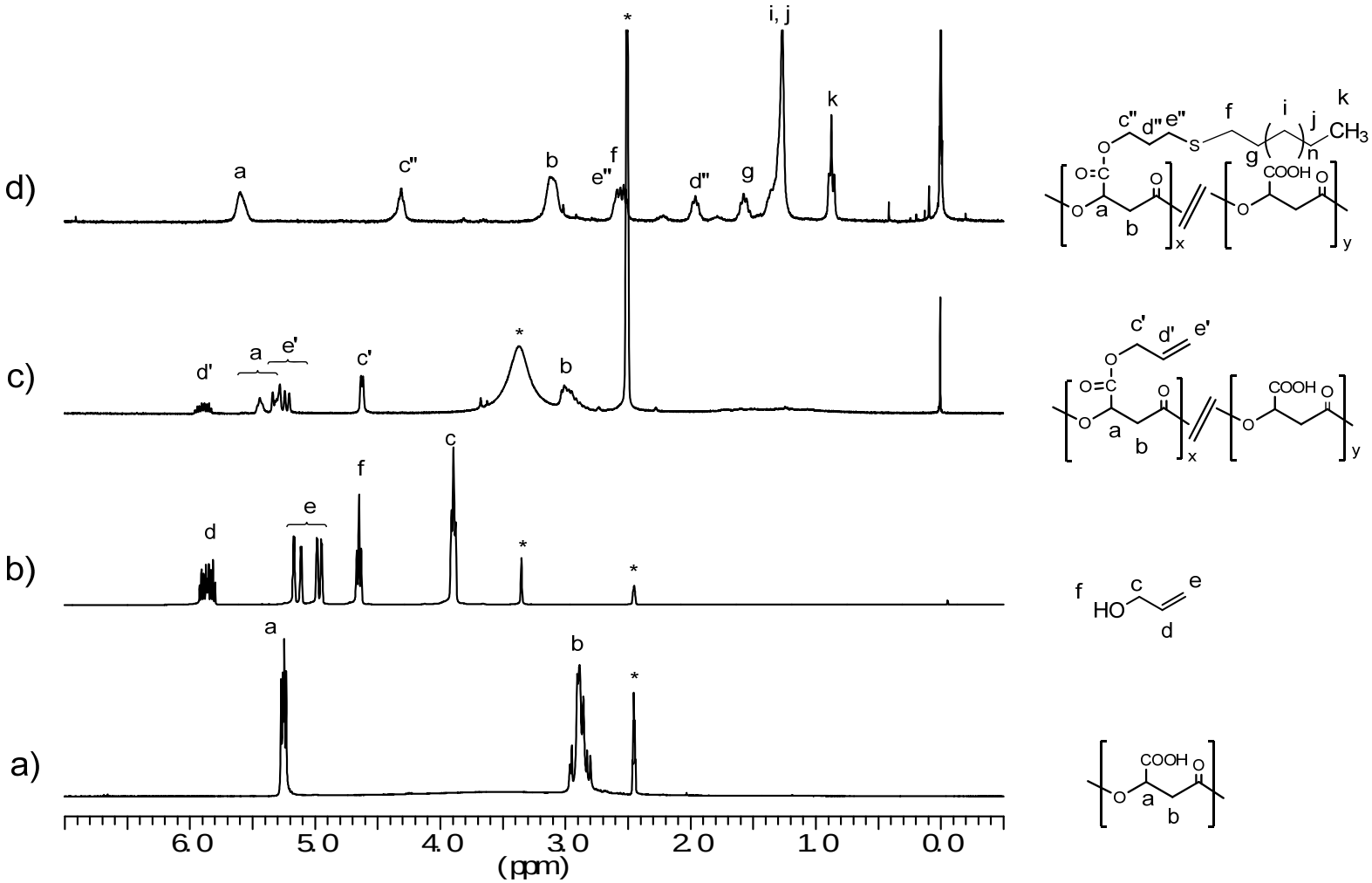
d)
c)
b)
a)
a
c''
b
e''
f
*
d''
g
i, j
k
d'
e'
c'
c
d
e
6.0
5.0
4.0
3.0
2.0
1.0
0.0
(ppm)
c'' d'' e''
f
i
j
k
CH3
S
n
COOH
O
x
y
HO

Figure 2

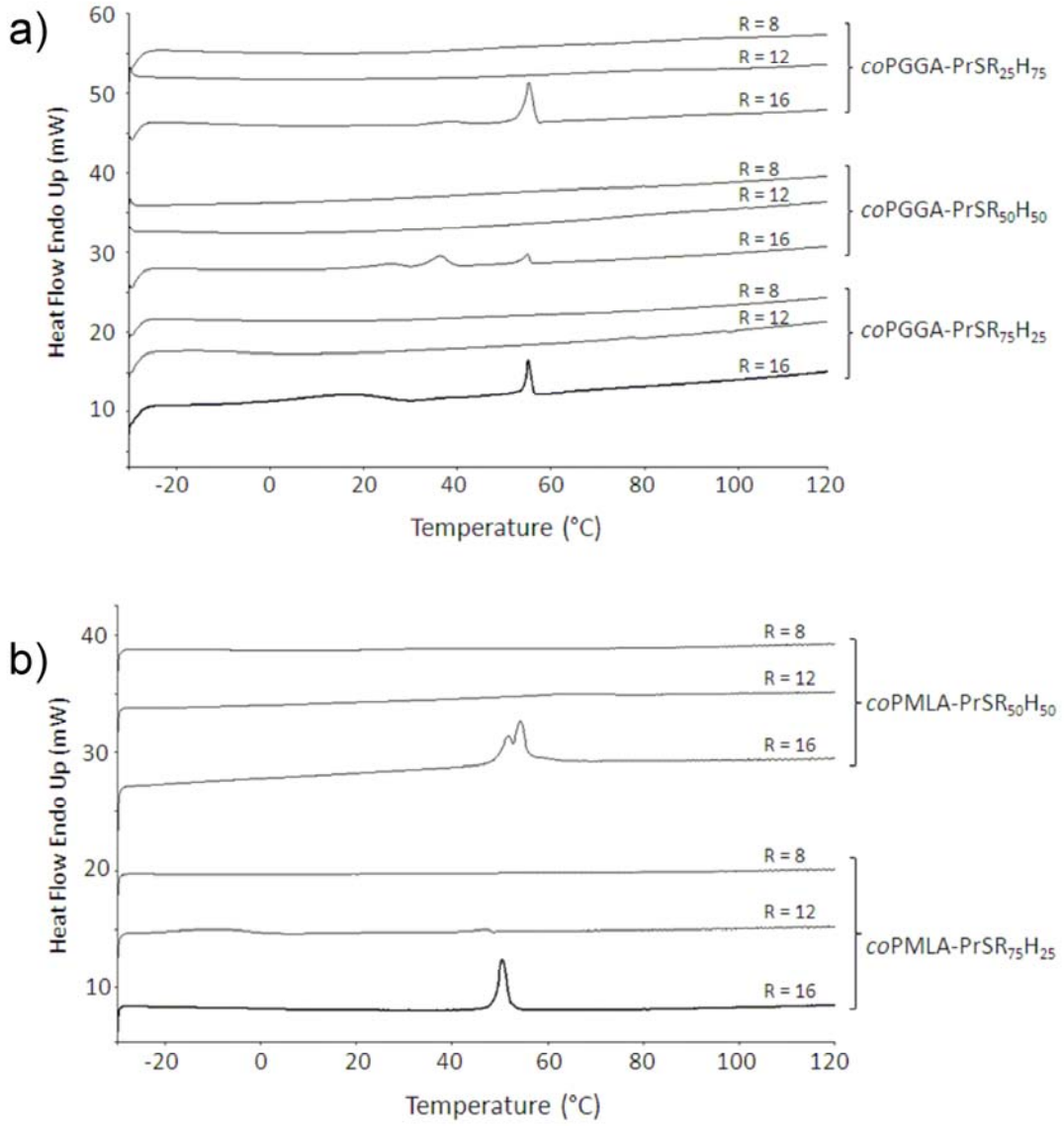
a)
Heat Flow Endo Up (mW)
Temperature (°C)
R = 8
R = 12
R = 16
coPGGA-PrSR25H75
coPGGA-PrSR50H50
coPGGA-PrSR75H25
b)
coPMLA-PrSR50H50
coPMLA-PrSR75H25

Figure 3.

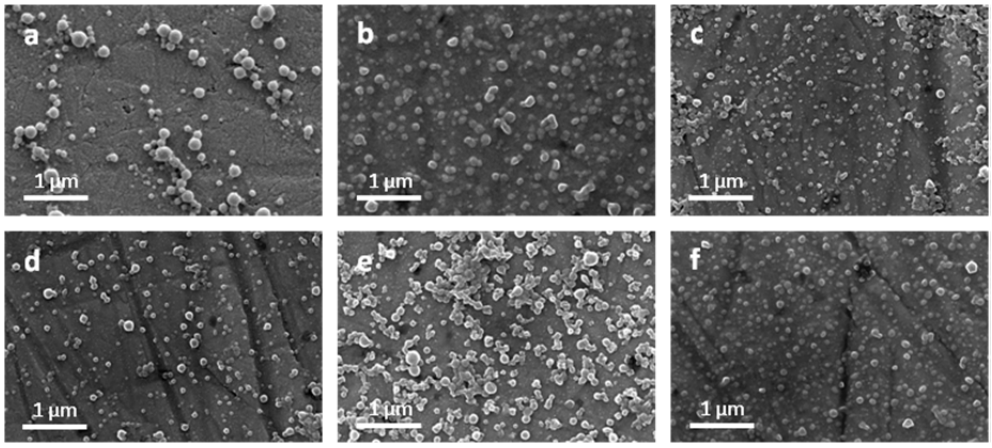

Figure 4

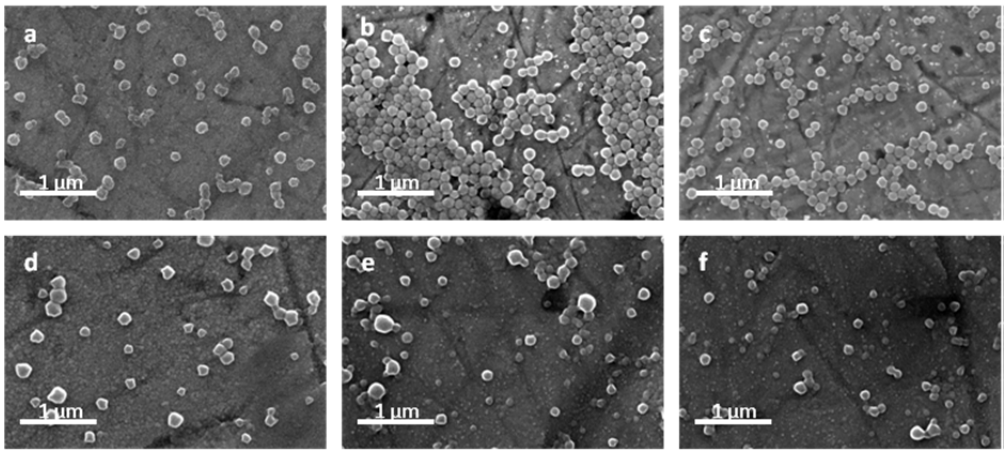

Figure 5

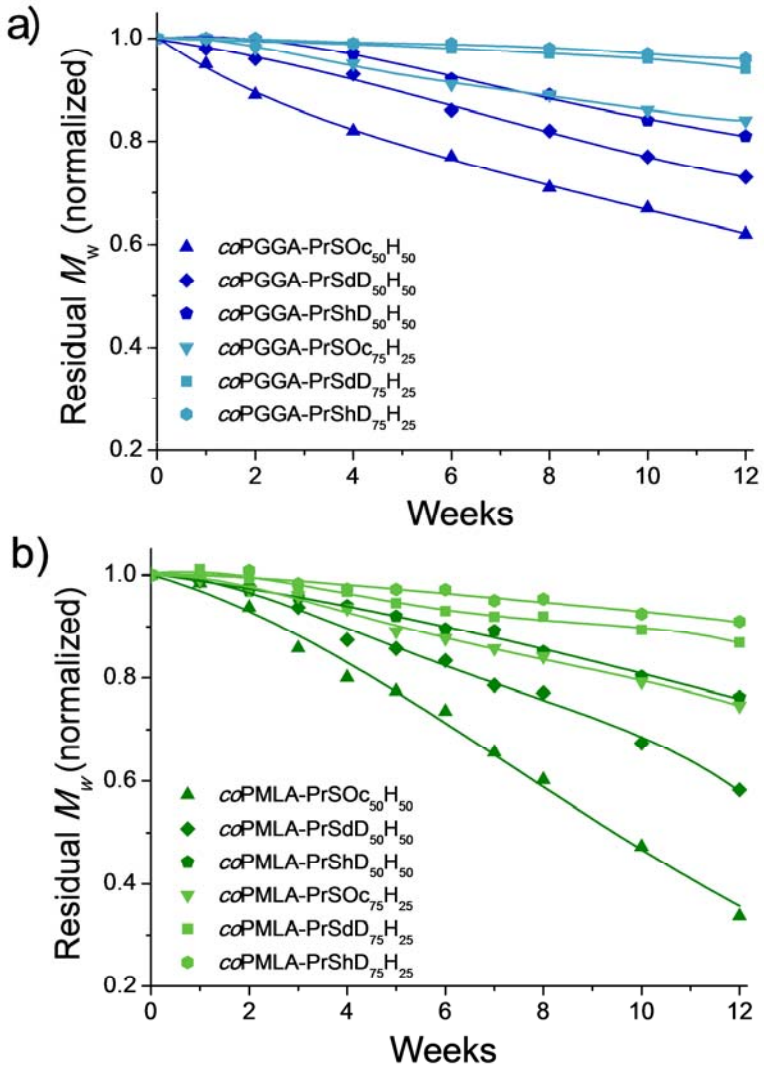
a)
Residual M_w (normalized)
1.0
0.8
0.6
0.4
0.2
0
2
4
6
8
10
12
Weeks
coPGGA-PrSOc50H50
coPGGA-PrSdD50H50
coPGGA-PrShD50H50
coPGGA-PrSOc75H25
coPGGA-PrSdD75H25
coPGGA-PrShD75H25
b)
Residual M_w (normalized)
1.0
0.8
0.6
0.4
0.2
0
2
4
6
8
10
12
Weeks
coPMLA-PrSOc50H50
coPMLA-PrSdD50H50
coPMLA-PrShD50H50
coPMLA-PrSOc75H25
coPMLA-PrSdD75H25
coPMLA-PrShD75H25

Figure 6

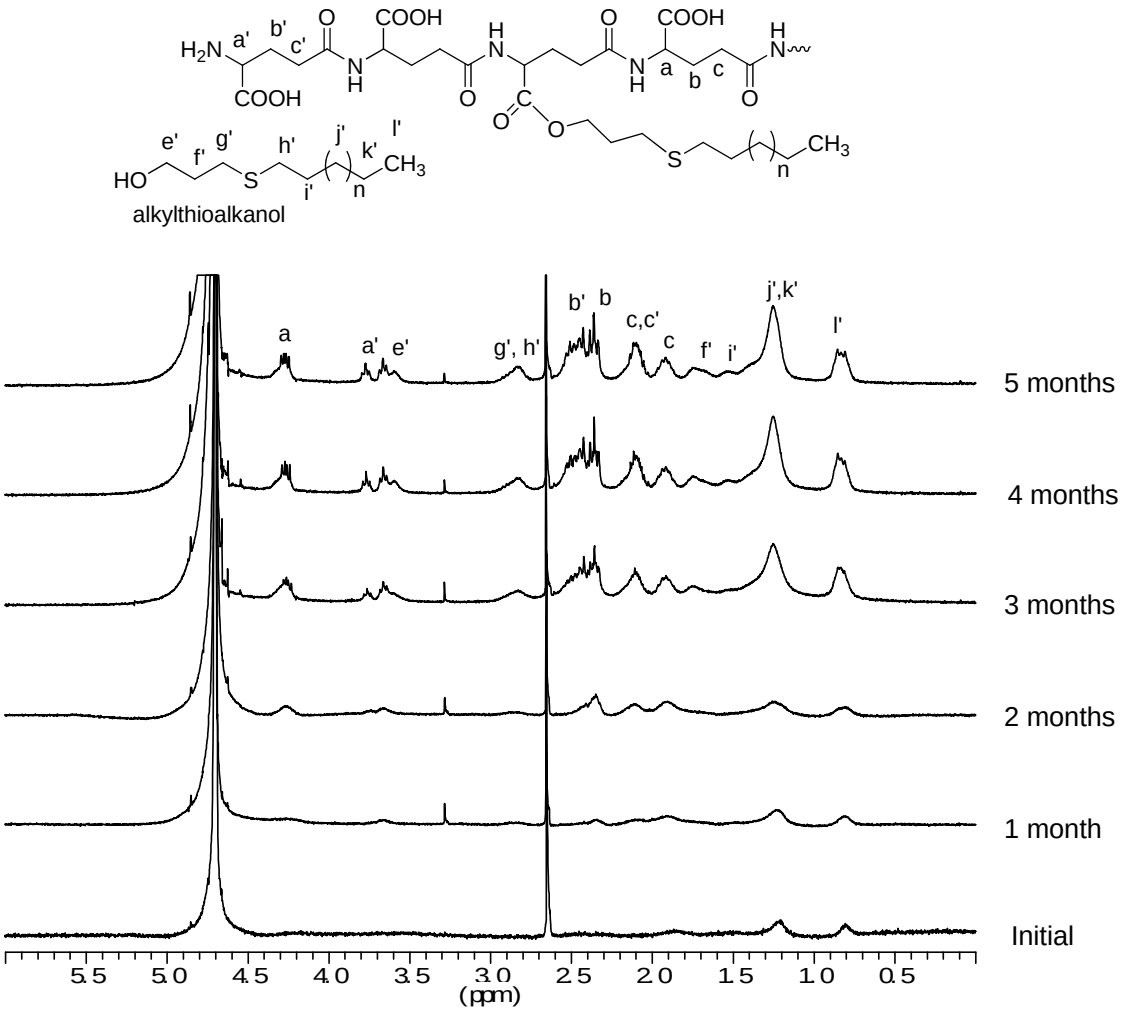
alkylthioalkanol
a
a' e'
g', h'
b' b
c,c'
c
f' i'
j',k'
l'
5 months
4 months
3 months
2 months
1 month
Initial
5.5 5.0 4.5 4.0 3.5 3.0 2.5 2.0 1.5 1.0 0.5
(ppm)

Figure 7

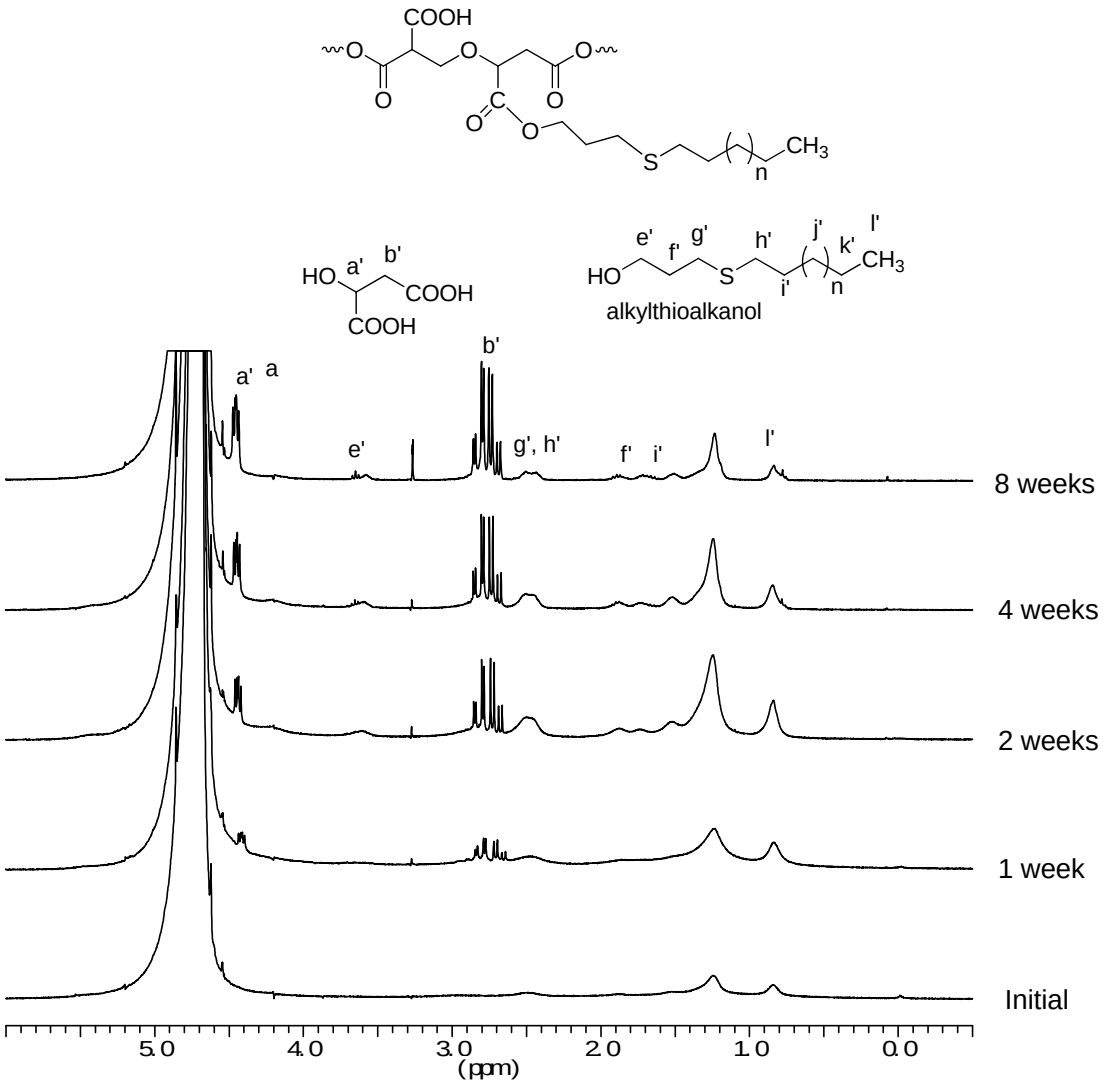
COOH
HO
a'
b'
COOH
COOH
alkylthioalkanol
e'
f'
g'
h'
j'
k'
l'
i'
n
CH3
a'
a
b'
e'
g', h'
f'
i'
l'
8 weeks
4 weeks
2 weeks
1 week
Initial
5.0
4.0
3.0
2.0
1.0
0.0
(ppm)

Figure 8

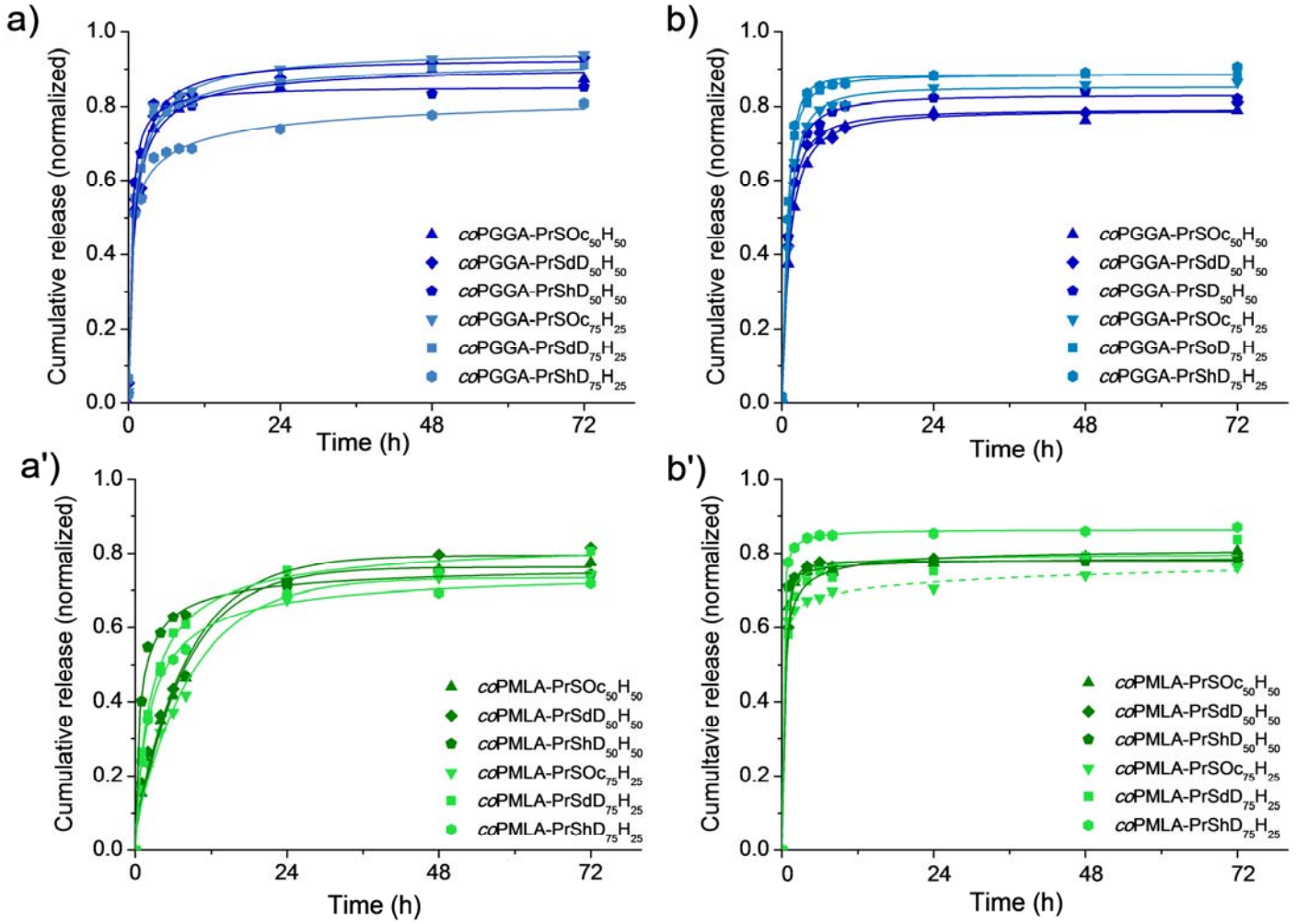
a)
b)
a')
b')
Cumulative release (normalized)
Cumultavie release (normalized)
Time (h)
0.0
0.2
0.4
0.6
0.8
1.0
0
24
48
72
coPGGA-PrSOc50H50
coPGGA-PrSdD50H50
coPGGA-PrShD50H50
coPGGA-PrSOc75H25
coPGGA-PrSdD75H25
coPGGA-PrShD75H25
coPGGA-PrSD50H50
coPGGA-PrSoD75H25
coPMLA-PrSOc50H50
coPMLA-PrSdD50H50
coPMLA-PrShD50H50
coPMLA-PrSOc75H25
coPMLA-PrSdD75H25
coPMLA-PrShD75H25

Figure 9

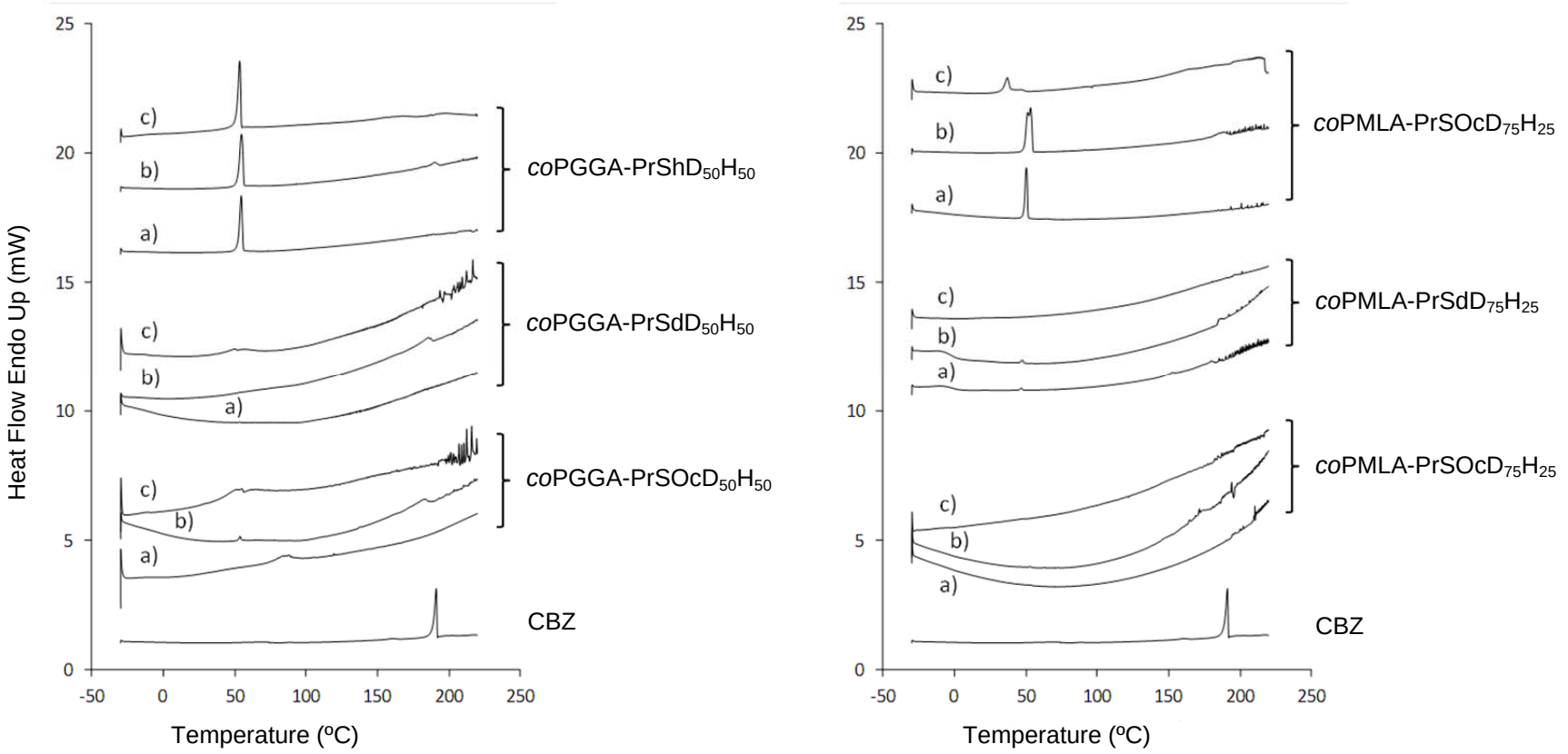
Heat Flow Endo Up (mW)
Temperature (ºC)
c)
b)
a)
coPGGA-PrShD50H50
coPGGA-PrSdD50H50
coPGGA-PrSOcD50H50
CBZ
coPMLA-PrSOcD75H25
coPMLA-PrSdD75H25
coPMLA-PrSOcD75H25
CBZ

Figure 10

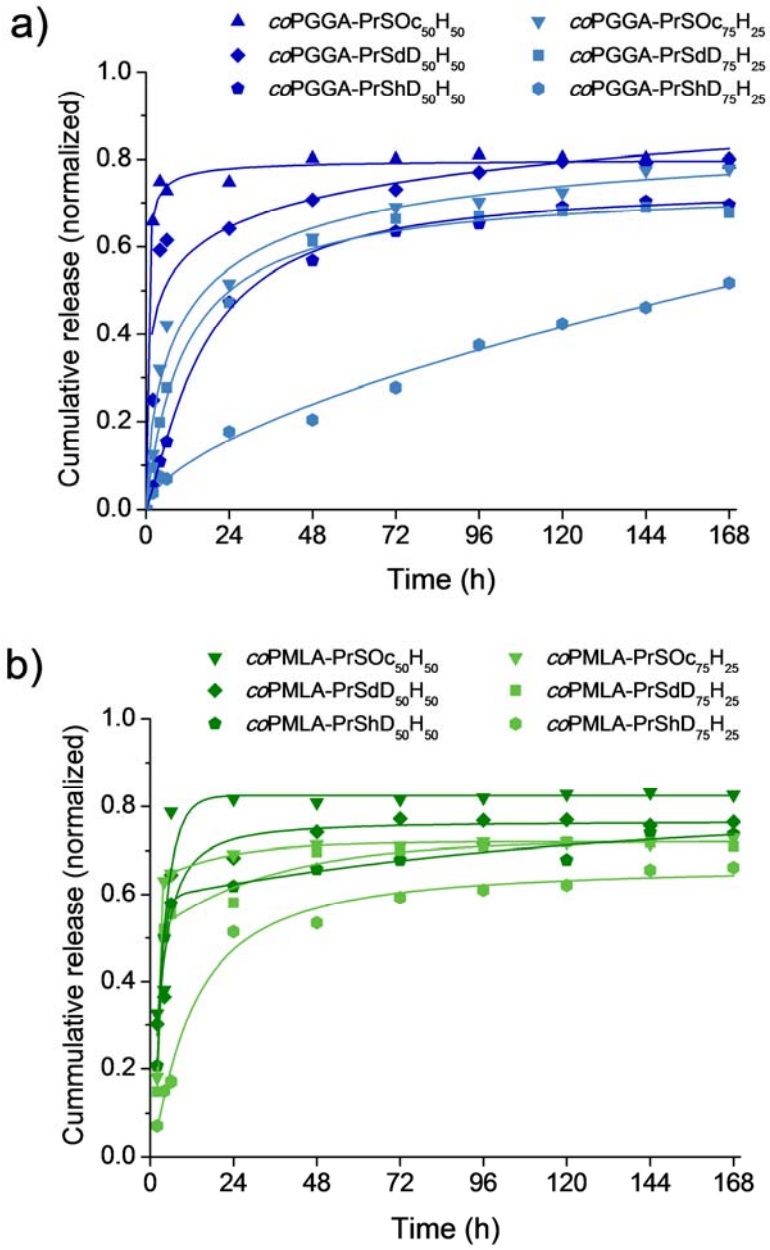
a)
coPGGA-PrSOc50H50
coPGGA-PrSdD50H50
coPGGA-PrShD50H50
coPGGA-PrSOc75H25
coPGGA-PrSdD75H25
coPGGA-PrShD75H25
Cumulative release (normalized)
Time (h)
b)
coPMLA-PrSOc50H50
coPMLA-PrSdD50H50
coPMLA-PrShD50H50
coPMLA-PrSOc75H25
coPMLA-PrSdD75H25
coPMLA-PrShD75H25
Cummulative release (normalized)
Time (h)

Figure 11

Table 1. Step 1: Reaction conditions, conversion degrees, yields and molecular weights obtained for the different polymers.

	Feed[a](mol:mol)	Esterification (%-mol)	Yield (%)	M_w[b]	$Đ$[b]
PGGA	-	-	-	30,000	-
*co*PGGA-$Al_{25}H_{75}$	1 : 0.25	26	88	30,600	2.9
*co*PGGA-$Al_{50}H_{50}$	1 : 0.50	55	96	37,900	2.3
*co*PGGA-$Al_{75}H_{25}$	1 : 0.75	73	92	44,200	2.6
PMLA	-	-	-	25,000	-
*co*PMLA-$Al_{50}H_{50}$	1 : 0.50	48	79	27,300	2.8
*co*PMLA-$Al_{75}H_{25}$	1 : 0.75	73	75	33,500	3.0

[a] Molar ratio of PGGA to allyl bromide or PMLA to DCC.
[b] Weight-average molecular weight and dispersity estimated by GPC.

Table 2. Step 2: Results of the thiol-ene *click* reaction on allylated PGGA and PMLA.

Polymer	Conversion %	Yield %	M_w[a]	$Đ$[a]
*co*PGGA-PrSOc$_{25}$H$_{75}$	100	61	25,200	2.5
*co*PGGA-PrSdD$_{25}$H$_{75}$	100	62	27,800	2.6
*co*PGGA-PrShD$_{25}$H$_{75}$	100	78	30,600	2.8
*co*PGGA-PrSOc$_{50}$H$_{50}$	100	67	29,000	2.9
*co*PGGA-PrSdD$_{50}$H$_{50}$	100	74	31,800	2.3
*co*PGGA-PrShD$_{50}$H$_{50}$	100	64	33,200	2.3
*co*PGGA-PrSOc$_{75}$H$_{25}$	100	60	30,300	2.6
*co*PGGA-PrSdoD$_{75}$H$_{25}$	100	79	33,700	2.8
*co*PGGA-PrShxD$_{75}$H$_{25}$	100	76	35,300	3.0
*co*PMLA-PrSOc$_{50}$H$_{50}$	100	49	31,000	2.1
*co*PMLA-PrSdoD$_{50}$H$_{50}$	100	49	32,100	2.2
*co*PMLA-PrShxD$_{50}$H$_{50}$	100	50	33,400	2.4
*co*PMLA-PrSOc$_{75}$H$_{25}$	100	51	33,100	2.0
*co*PMLA-PrSdoD$_{75}$H$_{25}$	100	47	36,300	2.4
*co*PMLA-PrShxD$_{75}$H$_{25}$	100	56	38,700	2.8

[a] Weight-average molecular weight and dispersity estimated by GPC.

Table 3. Nanoparticle characterization and drug content and encapsulation efficiency for Carbamazepine and Theophylline.

				CBZ		THEO	
	Size (nm)	I.D.[a]	ζ-pot (mV)	Cont. (%)	E.E. (%)	Cont. (%)	E.E. (%)
*co*PGGA-PrSOc$_{50}$H$_{50}$	194	0.408	-30.2	3.18	15.9	0.54	2.7
*co*PGGA-PrSdD$_{50}$H$_{50}$	157	0.294	-33.5	4.15	20.7	0.65	3.2
*co*PGGA-PrShD$_{50}$H$_{50}$	76	0.155	-32.1	7.68	38.4	1.74	8.7
*co*PGGA-PrSOc$_{75}$H$_{25}$	138	0.157	-29.9	5.36	26.8	2.70	13.5
*co*PGGA-PrSdD$_{75}$H$_{25}$	135	0.160	-28.4	3.38	16.9	1.99	9.9
*co*PGGA-PrShD$_{75}$H$_{25}$	144	0.203	-28.5	1.85	9.2	1.61	8.0
*co*PMLA-PrSOc$_{50}$H$_{50}$	197	0.383	-40.6	5.8	29.0	4.1	20.5
*co*PMLA-PrSdD$_{50}$H$_{50}$	236	0.544	-32.3	6.4	32.0	3.8	19.0
*co*PMLA-PrShD$_{50}$H$_{50}$	170	0.335	-29.0	6.9	34.5	2.8	13.9
*co*PMLA-PrSOc$_{75}$H$_{25}$	206	0.343	-35.3	5.9	29.5	1.7	8.5
*co*PMLA-PrSdD$_{75}$H$_{25}$	239	0.486	-24.8	5.7	28.5	1.1	5.5
*co*PMLA-PrShD$_{75}$H$_{25}$	151	0.348	-12.7	4.9	24.5	1.4	7.0

[a] Dispersity index of particle sizes.